PRINT ISSN 1119-8362
Electronic ISSN 2659-1502

Full-text Available Online at
https://www.ajol.info/index.php/jasem
http://www.bioline.org.br/ja

J. Appl. Sci. Environ. Manage.
Vol. 26 (12) 1977-1987 December 2022

Production of Biodiesel from the Transesterification of Waste Cooking Oil using Biobased Sulphonated Catalyst prepared from Coconut Shells

OYEDOH, EA; OKODUWA, GU; * MADOJEMU, GO; AKHABUE, CE

Department of Chemical Engineering, Faculty of Engineering, University of Benin, Benin City, Edo State, Nigeria

**Corresponding Author Email: madojemugregory@gmail.com*
Co-Authors Email:egheoyedoh@uniben.edu; gladysokoduwa9@gmail.com; christopher.akhabue@uniben.edu

ABSTRACT: This study investigated the effects of transesterification process factors on biodiesel yield from waste cooking oil using a biobased sulphonated catalyst made from waste coconut shells. The catalyst was characterized in terms of surface structure, elemental compositions, surface area, pore volume and pore size. Reaction duration was varied from 30 to 180 minutes, catalyst loading varied from 1 to 6 wt%, and reaction temperature varied from 45 to 65°C are among the transesterification process variables studied. The Box Behnken design (BBD) of response surface methods was used to design the transesterification reaction. The catalyst surface morphology revealed that it has an uneven pore structure while elemental composition revealed that it is mainly composed of CaO (17.32%), SiO_2 (21.40%), SO_3 (21.04%), and Al_2O_3 (13.68%). The catalyst surface area, pore volume, and pore size were determined to be 474.4 $m^2.g^{-1}$, 0.295 $cm^3.g^{-1}$, and 2.144 nm, respectively. Reaction time and temperature had significant effect on the biodiesel yield while the influence of catalyst dosage was minimal. After a reaction time of 147.73 minutes and a catalyst dosage of 2.18 wt % at a reaction temperature of 65°C, a maximum yield of 96.22 percent of biodiesel was produced. The predicted R^2 (0.9541) and actual R^2 (0.7705) values were found to be in good agreement. Due to the high output of biodiesel, waste cooking oil could be a low-cost biobased feedstock for biodiesel formulations. The characteristics of biodiesel made from waste cooking oil were comparable to those of conventional biodiesel.

DOI: https://dx.doi.org/10.4314/jasem.v26i12.12

Cite this paper as: OYEDOH, E. A; OKODUWA, G. U; MADOJEMU, G. O; AKHABUE, C. E. (2022). Production of Biodiesel from the Transesterification of Waste Cooking Oil using Biobased Sulphonated Catalyst prepared from Coconut Shells. *J. Appl. Sci. Environ. Manage.* 26 (12) 1977-1987

Dates: Received: 26 November 2022; Revised: 07 December 2022; Accepted: 19 December 2022;
Published Online: 31st December 2022

Keywords: Waste cooking oil; biodiesel; transesterification; response surface methodology; Box Behnken design

Researchers are focusing their attention on ecofriendly and sustainable biofuel substitutes for petroleum based fuels or fossil fuels due to the daily increase in global energy demand and the growing serious risk to the environment as a result of the consumption of fossil fuels (Kour *et al.*, 2019). Biofuels are excellent example of renewable energy that can be produced utilizing biological organisms and will eventually reduce reliance on fossil fuels. In contrast to the geopolitical, volatility, finite nature, and negative global repercussions of fossil fuel energy, biofuels are appealing and practical source of renewable energy. Suresh *et al*. (2018) claimed that biodiesel is the only conceivable alternative to petrodiesel and that it is a boon to the rapidly decreasing fossil fuel resources. The high cost of raw ingredients is the most significant economic barrier in biodiesel production (Quah *et al.*, 2019; Zhang *et al.*, 2014). Acid oils, such as non-edible vegetable oils, waste cooking oils, and others, are thus seen as attractive raw resources due to their lower cost (Bora *et al.*, 2018). Furthermore, waste oils have a number of advantages: they do not compete with food; the method recycles waste oils while lowering manufacturing costs, boosting biodiesel's economic competitiveness (Zhang *et al.*, 2018; Maneerung *et al.*, 2016). Biodiesel made from vegetable oil would be roughly 50% more expensive than biodiesel made from waste cooking oils (Phan

**Corresponding Author Email: madojemugregory@gmail.com* and Phan, 2008). Transesterification appears to be the best method for reducing viscosity and minimizing engine problems among the three basic routes for producing biodiesel from oils, when compared to heating and microemulsification (Boey *et al*., 2011). Coconut shell (Cocos nucifera) is common in Nigeria and belongs to the *Arecaceae family*. It's made of renewable resources (Prauchner and Roriguez-reinoso, 2012; Sani *et al*., 2015). Furthermore, coconut shell has a high carbon concentration, low ash content, and high strength and hardness, making it ideal for catalyst development (Hidayu and Muda, 2016; Endut *et al*., 2017). Many factors, including the free fatty acid and water content of the feedstocks, the amount of alcohol, the amount and type of catalyst, the reaction temperature, the mixing strength, and the reaction time, have been found to affect the biodiesel production process with short-chain alcohols and an alkali catalyst in previous studies. Adequately addressing and optimizing so many reaction components necessitates a massive number of studies, and this necessitates a large number of them. Response surface methodology (RSM) is a numerical tool that is frequently utilized in a variety of chemical processes for optimization studies (Tabaraki *et al*., 2014; Jabeen *et al*., 2015). It is a collection of mathematical techniques for describing the link between a number of different factors and one or more responses (Witek-Krowiak *et al*., 2014). It eliminates the one-factor-at-a-time strategy, which results in a large number of experimental runs and takes a long time. RSM can also examine the interaction effect of two or more variables on the answer, which helps to understand the process better. Aside from that, RSM allows the best level of elements to be determined in order to maximize the desired result (Choi *et al*., 2016; Endut *et al*., 2017). Biodiesel was produced from waste vegetable oil in this study utilizing a biobased sulphonated catalyst prepared from coconut shell biomass in a transesterification reaction. The central composite design of response surface methodology was used to design, analyze, and optimize the transesterification reaction.

MATERIALS AND METHODS

Materials collection: Waste cooking oil (WCO) and coconut shells were collected at a fast food restaurant and a market in Benin City, Edo State, Nigeria, respectively. Because of their abundance, WCO and coconut shells were chosen as raw materials for the synthesis of biodiesel in this study. Chemicals of analytical grade were purchased locally and utilized without further purification.

Preparation and characterization of coconut shell sulphinated catalyst (CSSC): CSSC was prepared using methods by Endut *et al*. (2017) and Akhabue *et al*. (2020). The biomass was first cleaned with distilled water to eliminate contaminants before being sliced into 2 mm pieces and sun-dried for three days. To remove any moisture, the sliced biomass was dried in an oven at 100°C for 12 hours. About 20 g of the precursor carbon catalyst was partially carbonized at 280°C in a muffle furnace and then pre-treated with phosphoric acid for 72 hours before being decanted and washed with warm and cold distilled water to remove impurities and free ions. The carbonized sample was then pulverized to a fine powder (0.5–1 mm) in a laboratory mortar. In a 250 ml conical flask, 10 g carbon catalyst was mixed with 100 ml H_2SO_4 for 15 minutes to sulfonate the coconut shell carbon. The excess acid was eliminated by washing. The remaining wet particles (carbon and acid) were then transferred to a ceramic crucible in a muffle furnace and heated to a certain temperature for a predetermined amount of time. The sulfonated carbon catalyst was washed with extra distilled water until the wash water became neutral, then dried in an air-drying oven at 105°C for 10 hours after cooling to ambient temperature. To avoid contamination, the coconut shell sulfonated catalyst (CSSC) was maintained in an airtight container. CSSC was characterized in terms of functional groups using Fourier Transform Infrared (FTIR) spectroscopy, elemental composition using X-ray fluorescence (XRF) spectroscopy, surface area and pore diameter using Brunauer Emmett Teller (BET) technique, crystalline structure and phase using X-ray diffraction (XRD) technique and surface morphology using scanning electron microscope (SEM).

Transesterification reaction/Design of reaction: The transesterification reaction was carried out according to Mitaphonna *et al*. (2019) procedure. At 50°C, 50 g of WCO was heated for 30 minutes. During the transesterification procedure, the optimum methanol:oil ratio of 7:1 determined by Uddin *et al*. (2013) was maintained. The transesterification process variables and range of conditions include reactime of 30 - 180 mins, catalyst dosage of 1 - 6 wt% and temperature of 45 - 65°C. WCO was dissolved in methanol and agitated for 15 minutes with a magnetic stirrer. CSSC was added in varied levels depending on the experimental design. The combination was then injected into WCO. All of the materials were combined in a three-neck flask that was placed on a set of reflux apparatus that included a thermometer and a magnetic stirrer. For the various reaction times, the transesterification reaction was carried out at varied temperatures and agitated with a magnetic stirrer. The transesterification reaction was left to sit for 24 hours, until two layers developed. The methyl ester layer was on top, and glycerol was at the bottom. Equation (1) was used to compute the % biodiesel yield (BWCO).

$$BWCO\ yield\ (\%) = \frac{weight\ of\ BWCO}{weight\ of\ WCO} \times 100\% \quad (1)$$

The response pattern was studied and the best combination of factors was determined using a Box–Behnken Design (BBD) with three variables with three levels. For the experimental response of BWCO yield, a total of 17 trials were conducted individually. The conditions were chosen based on preliminary research conducted by Aisabor *et al*. (2016) and Mitaphonna *et al*. (2019). The percentage biodiesel yield was used as the trasesterification process dependent variable (response) . The coefficients of determination and analysis of variance were used to assess the model's fit (ANOVA) using Design Expert software (Stat-Ease, Inc., Minneapolis, MN, USA).

Analysis of WCO and BWCO: The following physico-chemical properties of the WCO and BWCO were determined using standard experimental procedures.

Density determination: The densities of WCO and BWCO were measured by relative density (R.D) bottle with a capacity of 10 ml and were determined using Equation (3).

$$Density = \frac{mass\ of\ oil\ sample\ (m)}{volume\ of\ the\ R.D\ bottle\ (V)} g/ml \quad (3)$$

Viscosity determination: The viscosity of a fluid is a measurement of its flow resistance. At 40°C, the viscosity of the oil and biodiesel was measured to see how they flowed. The OFITE automatic viscometer was used to perform the viscosity tests in accordance with ASTM D 445 (Saeed *et al*., 2019).

Acid value: WCO and BWCO acid values were determined using a titrimetric method according to AOAC (Association of Official Analytical Chemists) protocol (2000). In a 250 ml conical flask, 5 g of WCO and BWCO were measured. The mixture was then mixed with 25 mL of neutral ethyl alcohol and heated over a water bath. The mixture was titrated against a standard potassium hydroxide solution with shaking after adding a phenolphthalein indicator solution (1-2 drop). The first pink color which lasted for 30 seconds was marked as the termination point (Ekwu and Nwagu, 2004). Acid value was calculated as mg of KOH per gm of oil samples using Equation (4).

$$Acid\ value = \frac{V \times N \times 56.1}{W} \quad (4)$$

V=Volume of standard KOH solution in ml, N=Normality of standard KOH solution and W=Weight of WCO/BWCO samples in grams.

Percentage free fatty acid (FFA): The acid value is equivalent to the percent free fatty acid multiplied by the factor of 1.986, when the percent free fatty acid is based upon oleic acid as reported by (Adefarati, 1986).

Flash point: A substance's flashpoint is defined as the lowest temperature at which the substance experiences ignition upon application of an ignition source. WCO and BWCO flashpoints were determined using the Penskay-matrix testing device at 84℃ by ASTM D92 standard (Thushari and Babel, 2018).

Saponification value: The saponification value was calculated by placing 1.0 g each of oil WCO and BWCO in a conical flask and adding 25 ml 0.5N alcoholic KOH, which is heated for 30–40 minutes under a reserved condenser to guarantee that the sample is completely dissolved. After cooling the sample, phenolphthalein was added and titrated with 0.2N HCl until the sample reached a pink end point. The same time conditions were used to determine a blank. The saponification value was determined using Equation (5).

$$Saponification\ value = \frac{(Blank - titre) \times 56.1}{weight\ of\ oil\ (g)} \quad (5)$$

Iodine value: The number of centigrams of iodine absorbed per gram of sample is known as the iodine value, which is a measure of the unsaturation of fatty acids (% iodine absorbed). Wijs technique (British standard BS 684: Section 2.13:1976) was used to determine the iodine values of oil and biodiesel samples (Salimon *et al*., 2012). To assess the unsaturation of the compounds, 0.5 g of WCO and BWCO were utilized. To dissolve the oil, 15 mL of carbon tetrachloride was added, followed by 25 mL of Wijs reagent. After that, a cork was inserted, and the flask's contents were gently shaken. After that, the flask was placed in the dark for 30 minutes. A stopper was then inserted and the content of the flask was shaken gently. The flask was then placed in the dark for 30 mins. At the end of this period, 20 ml of 10% aqueous potassium iodide and 150 ml of distilled water were added using a measuring cylinder. The content was titrated with 0.1M sodium thiosulphate solution until the yellow color almost disappeared. A few drops of starch indicator were added and the titration continued by adding sodium thiosulphate drop-wise until blue coloration disappeared after vigorous shaking. The above process was repeated with a blank under the same conditions. The iodine value (IV) is given by the expression:

$$IV = 12.69 \times T \times (V_1 - V_2)/m \qquad (6)$$

Where V_1 = Volume of sodium thiosulphate used for the blank, V_2 = Volume of sodium thiosulphate used for the test portion, T = Normality of sodium thiosulphate used, m = Mass in g, of the test portion.

RESULTS AND DISCUSSIONS

Characteristics of coconut shell sulphonated catalyst: The elemental composition of CSSC as analyzed using XRF machine indicate CSSC is mainly composed of Al_2O_3 (13.6771%), SiO_2 (21.3975%), SO_3 (21.0405%), CaO (17.3249), P_2O_5 (0.7437%), K_2O (0.5519%) and Fe_2O_3 (0.2911%). The presence of the metal oxides indicates the efficiency of CSSC to be used in catalytic processes. The transition metals and their compounds are used as catalyst because of their ability to change oxidation state or in the case of the metals, to adsorb other substances on their surface as catalyst. Figure 1 shows the SEM micrograph of CSSC at 750 resolutions. CSSC has a highly developed and uneven pore structure, which reveals enormous pore sizes in the CSSC particles, as can be observed in the micrograph. The big holes in the CSSC could be due to sulphonation of the catalyst, which increases the number of active sites in a catalyst and hence improves the surface area for greater catalyst performance. CSSC has a BET surface area of 474.4 $m^2.g^{-1}$, as estimated using the BET technique. The pore volume was found to be 0.295 $cm^3.g^{-1}$, with a pore diameter of 2.144 nm. As indicated, the BET surface area is the primary indicator of activated carbon/catalyst surface attributes as described by Chandra *et al*. (2009) and Kalderis *et al*. (2008). The high surface area of 474.4 $m^2.g^{-1}$ of CSSC calculated by the BET method indicates the possibility of applying the CSSC in catalytic reactions. According to the International Union of Pure and Applied Chemistry (IUPAC), the pore development of an activated carbon/catalyst is classified into three groups which are micropores (size < 2 nm), mesopores (2–50 nm) and macropores (size > 50 nm) (Mohd Iqbaldin *et al*., 2013). The pore size of 2.144 nm of CSSC falls within the mesoporous pore size distribution.

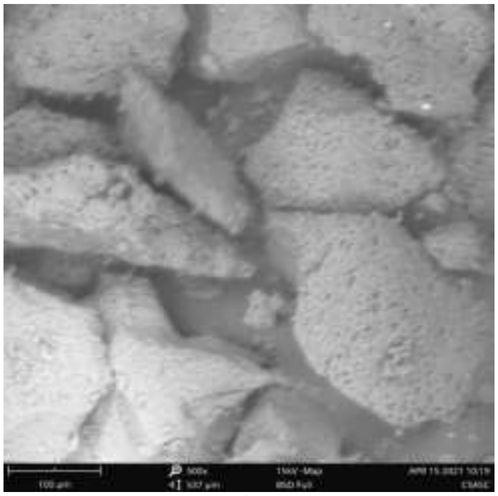

Fig 1: SEM micrograph for CSSC at 750 resolution

Biodiesel (BWCO) yield: The BBD combination of transesterification process variables, the actual and predicted percentage yield of biodiesel of waste cooking oil (BWCO) obtained from CSSC catalyzed transesterification reaction of WCO are given in Table 1. As seen in Table 1, the maximum percentage yield of BWCO obtained from the CSSC catalyzed transesterification reaction of WCO is 90.13%.

Table 1: Experimental design matrix of transesterification reaction with yields of BWCO

Run order	**Coded factors**			**Actual factors**				**BWCO yield (%)**
	A	**B**	**C**	**Reaction time (mins)**	**Catalyst dosage (wt. %)**	**Reaction temperature (℃)**	**Actual**	**Predicted**
1	0	0	0	105	3.5	55	85.67	86.42
2	0	1	-1	105	6.0	45	75.98	73.32
3	-1	1	0	30	6.0	55	55.81	58.37
4	1	0	1	180	3.5	65	90.13	90.03
5	1	1	0	180	6.0	55	66.66	66.65
6	0	0	0	105	3.5	55	83.19	86.42
7	-1	-1	0	30	1.0	55	47.77	47.78
8	0	0	0	105	3.5	55	87.32	86.42
9	1	0	-1	180	3.5	45	70.17	72.84
10	-1	0	-1	30	3.5	45	56.71	56.81
11	0	-1	1	105	1.0	65	85.00	87.66
12	1	-1	0	180	1.0	55	88.79	86.23
13	0	-1	-1	105	1.0	45	81.11	81.00
14	-1	0	1	30	3.5	65	61.99	59.32
15	0	1	1	105	6.0	65	86.24	86.35
16	0	0	0	105	3.5	55	86.78	86.42
17	0	0	0	105	3.5	55	89.12	86.42

The actual versus predicted plot of the CSSC catalyzed transesterification reaction of WCO to produce biodiesel is shown in Figure 2.

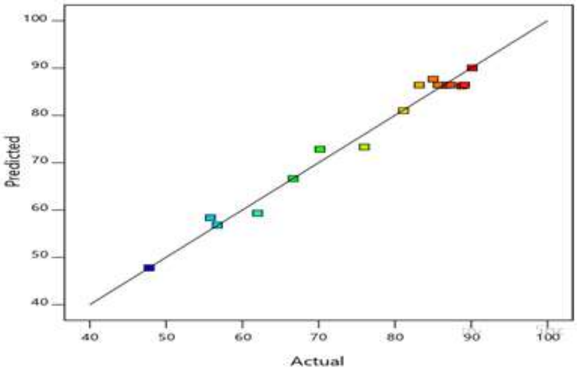

Fig 2: Actual vs. predicted plot of BWCO yield

From the plot, it can be seen that a positive strong correlation exist between the actual and predicted values of the percentage BWCO yield. The model summary statistics of the BWCO yield from WCO transesterification is given in Table 2. The coefficient of regression, R^2 was used to validate the fitness of the model equation. A higher R^2 value close to unity gives a better model. From Table 2, the cubic source of variability gave a higher R^2 value (0.9937) but the cubic model is usually aliased from response surface methodology making the quadratic source of variability with a higher R^2 value (0.9799) than the two factor interaction (2FI) and linear sources of variation the best to evaluate the fitness of the model of the transesterification process.

Table 2: Model summary statistics of transesterification reaction

Source	Std. Dev.	R^2	Adjusted R^2	Predicted R^2	PRESS	
Linear	11.44	0.4380	0.3083	-0.0100	3058. 84	
2FI	11.88	0.5342	0.2548	-0.7008	5151.04	
Quadratic	**2.95**	**0.9799**	**0.9541**	**0.7705**	**695.04**	**Suggested**
Cubic	2.19	0.9937	0.9746		*	Aliased

The analysis of variance for the quadratic model of the percentage BWCO yield from the CSSC catalyzed transesterification reactions of WCO is given in Table 3 at a significant level of 5% (probability of error of 0.05). From Table 3, the model F-value of 37.97 and a very low p-value of <0.0001 implies the model is significant on the percentage BWCO yield from the transesterification reactions. There is only a 0.01% chance that an F-value this large could occur due to noise. P-values less than 0.0500 indicate model terms are significant. In this case, reaction time (A), reaction temperature (C), interaction factors (AB and AC), and quadratic factors (A^2 and B^2) are significant model terms (i.e. change in their values leads to a corresponding change in the percentage BWCO yield). The other factors, catalyst dosage (B), interaction (BC) and quadratic factor (C^2) have insignificant effects on the percentage BWCO yield. The Lack of Fit F-value of 2.88 and high p-value (0.1664) greater than 0.0500 implies the Lack of Fit is not significant relative to the pure error. There is a 16.64% chance that a Lack of Fit F-value this large could occur due to noise. Non-significant lack of fit is desirable, it indicate model is fit.

Table 3: ANOVA for quadratic model of percentage BWCO yield

Source	Sum of Squares	df	Mean Square	F-value	p-value
Model	2967.85	9	329.76	37.97	< 0.0001*
A – Reaction time	1092.08	1	1092.08	125.76	< 0.0001*
B – Catalyst dosage	40.41	1	40.41	4.65	0.0679
C – Reaction temperature	193.95	1	193.95	22.33	0.0021*
AB	227.56	1	227.56	26.20	0.0014*
AC	53.88	1	53.88	6.20	0.0415*
BC	10.14	1	10.14	1.17	0.3156
A^2	1216.20	1	1216.20	140.05	< 0.0001*
B^2	91.55	1	91.55	10.54	0.0141*
C^2	0.4571	1	0.4571	0.0526	0.8251
Residual	60.79	7	8.68		
Lack of Fit	41.56	3	13.85	2.88	0.1664
Pure Error	19.22	4	4.81		
Cor. Total	3028.64	16			

The empirical relationship between the transesterification reaction variables considered and the percentage yield BWCO in coded units is given by Equation (7) for the CSSC catalyzed transesterification reactions of WCO.

$$BWCO\ yield\ (\%) = 86.42 + 11.68A - 2.25B + 4.92C - 7.54AB + 3.67AC + 1.59BC - 17.00A^2 + 4.66B^2 + 0.33C^2 \qquad (7)$$

Equation (7) in terms of coded factors can be used to make predictions about the response (% biodiesel yield) for given levels of each independent variable. The coded equation is useful for identifying the relative impact of the independent variables by comparing their coefficients. Factors with positive coefficient have positive effect on the response variables (i.e. increase or decrease in their values will lead to a corresponding increase or decrease in the response and vice versa) while factors will negative coefficients have negative effects (i.e. increase or decrease in factors with negative coefficients will lead to decrease or increase in the response variable). Among the main factors, reaction time and reaction temperature were found to have positive effects on the percentage BWCO yield (positive coefficients) while catalyst dosage had negative effect (negative coefficient) on the percentage biodiesel yield from the CSSC catalyzed transesterification reaction of WCO. The interaction of reaction time and catalyst dosage (AB) had negative effect on the percentage BWCO yield while other interaction factors (AC and BC) had positive effects. A^2 had negative effect on the percentage BWCO yield while B^2 and C^2 had positive effects on the percentage BWCO yield. Reaction time (A) had the highest effect on the percentage BWCO yield (with highest coefficient of 11.68) while catalyst dosage (B) had the least effect with lowest coefficient of 2.25 among the main factors. The goodness of the regression model can further be described using the Fit statistics given in Table 4. Standard deviation is expressed as a percentage of the mean in coefficient of variation (CV). Reproducibility is improved by lower CV values. In general, a high CV suggests that there is a lot of variance in the mean value and that the response model isn't developing properly. The CV is 3.86 percent, which is within acceptable limits. The model was found to have a very high R^2 value of 0.9799, indicating that it can account for 98 percent of the variability in percentage biodiesel yield. The adjusted R^2 of 0.9541 is reasonably close to the expected R^2 of 0.7705, i.e. the difference is less than 0.2. This shows that employing a quadratic polynomial to represent the transesterification process was effective utilizing response surface approach. The signal-to-noise ratio is measured with adequate precision. It is preferable to have a ratio of more than four. Your signal-to-noise ratio of 18.693 suggests a good signal. The design space can be navigated using this concept.

Table 4: Fit statistics of regression model

Standard Deviation (%)	2.95	R^2	0.9799
Mean (%)	76.38	Adjusted R^2	0.9541
Coefficient of variation, CV (%)	3.86	Predicted R^2	0.7705
		Adequate Precision	18.6930

The effects of interaction of the transesterification process variables considered on the percentage BWCO yield is shown in Figure 3. Figure 3 (a) shows the effect of reaction time and catalyst dosage on percentage BWCO yield. It can be seen that increase in the reaction time and catalyst dosage lead to decrease in the percentage BWCO yield at constant reaction temperature. The effect of reaction time and temperature is shown in Figure 3 (b). It can be seen that increase in the reaction time and reaction temperature at constant catalyst dosage lead to increase in the percentage BWCO yield. Figure 3 (c) shows the effect of catalyst dosage and reaction temperature on the percentage BWCO yield at constant reaction time. Increase in the catalyst dosage and reaction temperature lead to increase in the percentage BWCO yield. The effect of reaction time was more pronounced as seen in Figures 3 (a) and (b) while catalyst dosage produced the least effect on the percentage BWCO yield as seen in Figures 3 (b) and (c). From the numerical optimization studies, the maximum percentage yield of BWCO of 96.22% was obtained after a transesterification reaction time of 147.73 mins using catalyst dosage of 2.18 wt% at a transesterification reaction temperature of 65°C. The achieved maximum desirability of 0.924 indicate that the possibility of reaching over 92% of the maximum possible percentage yield of BWCO.

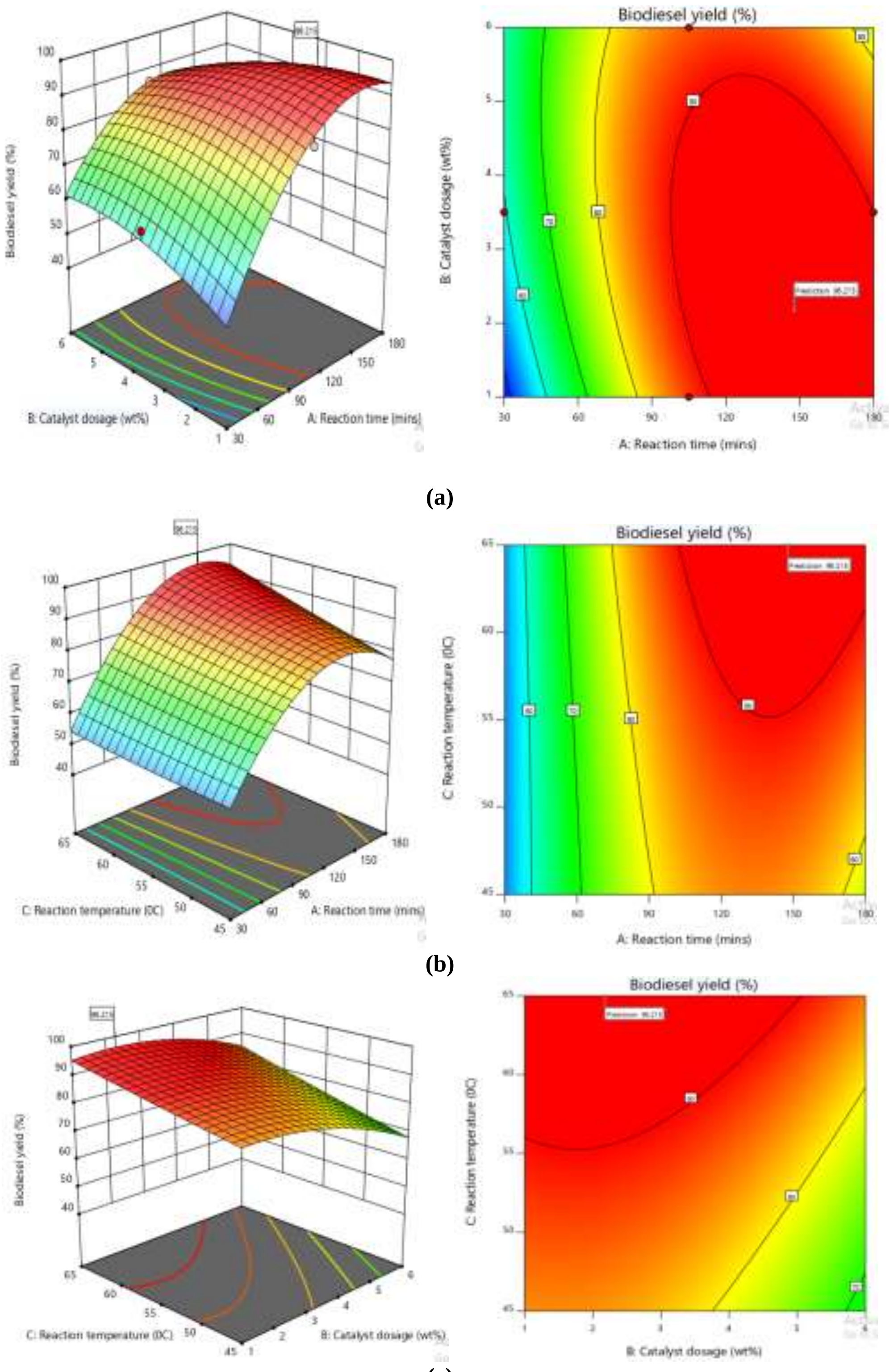

(a)

(b)

(c)

Fig 3: Effect of interaction of transesterification process variables on percentage yield of biodiesel (a) reaction time and catalyst dosage (AB), (b) reaction time and reaction temperature (AC) and (c) catalyst dosage and reaction temperature (BC)

The physicochemical properties of WCO and BWCO are given in Table 5. The properties of BWCO were compared to the ASTM6751 and EN14214 standards of biodiesel. It can be observed from Table 5 that the viscosity of BWCO was within the ASTM 6751 standard but slightly above the EN14214 standard of biodiesel. The density of BWCO was within the EN14214 standard of biodiesel. The acid value was above both the ASTM 6751 and EN14214 standards of biodiesel. The iodine value was far less than the EN14214 standard while flash point of BWCO was within the range specified by both the ASTM 6751 and EN14214 standards of biodiesel. Figure 4 shows the GCMS of WCO. Table 6 gives the fatty acid profile of WCO as given by GCMS. Table 7 gives the functional groups in WCO as analyzed by the FTIR machine at a wavelength of 4000 – 650 cm^{-1}.

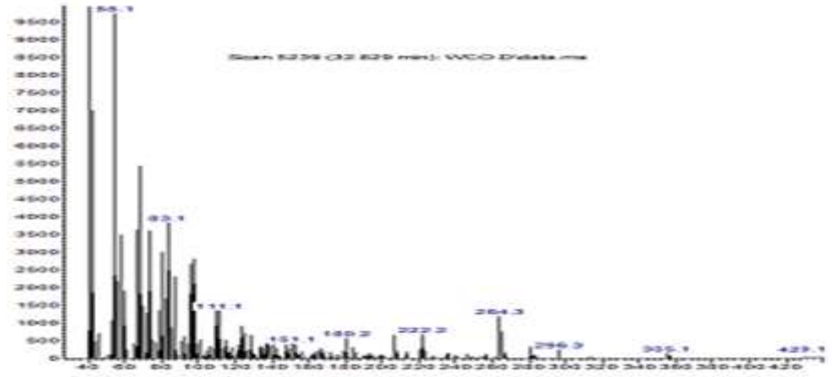

Fig 4: GCMS of WCO

Table 5: Physicochemical properties of WCO and BWCO and comparison with standards

Properties	WCO	BWCO	ASTM D6751	EN 14214
Viscosity @ 40^{0}C (mm^2.s^{-1})	7.0	5.2	1.9 to 6.0	3.5 to 5.0
Density (g.L^{-1})	920	898	-	860 to 900
Saponification Value (mg KOH.g^{-1})	243.42	131	-	-
Acid Value (mg KOH.g^{-1})	7.85	2.02	0.5 max	0.5 max
FFA (%)	3.94	1.02	-	-
Molecular mass (g.mol^{-1})	712.44	541.29		
Iodine Value (g.[100g]$^{-1}$)	35.97	12.47	-	120 max
Flash Point (℃)	135	251	>130	>120

Table 6: Fatty acid profile of WCO

Peak	Fatty acids	Retention time	Area (%)
1	Dodecanoic acid	25.6895	5.8184
2	Pentadecane, 2,6,10,14-tetramethyl-	29.0941	6.9455
3	Tetradecanoic acid	29.7574	7.1543
4	N,N-Dimethyldodecanamide	30.4905	1.2578
5	Linoelaidic acid	30.5885	0.5303
6	9,17-Octadecadienal, (Z)-	30.7756	2.615
7	Cyclooctene, 3-ethenyl-	30.8071	0.6187
8	13-Octadecenal, (Z)-	30.8806	1.4574
9	9,12-Octadecadien-1-ol, (Z,Z)-	30.9598	2.9516
10	Hexadecanoic acid, methyl ester	31.4742	1.2352
11	Palmitoleic acid	31.6867	7.6679
12	n-Hexadecanoic acid	31.8731	16.4028
13	Oleic Acid	32.0533	0.7985
14	Oleic Acid	32.1506	0.2448
15	Oleic Acid	32.2549	0.4943
16	Oleic Acid	32.3086	0.4738
17	Octanamide, N,N-dimethyl-	32.3902	0.8074
18	2-Methyl-Z,Z-3,13-octadecadienol	32.5502	0.2851
19	9,12-Octadecadienoic acid (Z,Z)-	32.7696	1.1733
20	11-Octadecenoic acid, methyl ester	32.8294	2.3171
21	2,5-Dihydroxybenzoic acid, 3TMS derivative	32.8768	0.7167
22	Heptadecanoic acid, 16-methyl-, methyl ester	33.0298	1.0569
23	cis-Vaccenic acid	33.1792	25.5431
24	Octadecanoic acid	33.3341	3.0255
25	Octanamide, N,N-dimethyl-	33.9002	0.7406
26	1,5,9-Undecatriene, 2,6,10-trimethyl-, (Z)-	34.1269	1.2562
27	9,12,15-Octadecatrien-1-ol, (Z,Z,Z)-	34.4031	2.264
28	Octadec-9-enoic acid	34.6479	1.4954
29	9-Octadecenamide, N,N-dimethyl-	35.3393	0.6931
30	2,3-Dihydroxypropyl elaidate	36.0606	1.9594

Table 7: Functional groups of WCO

S/No.	Frequency (cm^{-1})	Appearance	Bonds	Compounds
1.	3011.7	Strong and broad absorption band	O-H stretching	Carboxylic acids
2.	2922.2	Strong absorption band	C-H stretching	Alkanes and alkyls
3.	2855.1	Strong absorption band	C-H stretching	Alkanes and alkyls
4.	1744.4	Strong absorption band	C=O stretching	Five member cyclic ketones, or ester (R-C(O)-O-R)
5.	1461.1	Strong absorption band	C-H bend, ring C=C stretch	Alkanes and alkyls, Ar. Compounds
6.	1375.4	Medium absorption band	CH_3C-H bend	Alkanes and alkyls
7.	1230.0	medium strong absorption band	=C-O-C sym.	Ar-O-R
8.	1151.7	Very strong absorption band	C-F stretch	R-F
9.	1114.5	Very strong absorption band	C-F stretch	R-F
10.	965.4	Strong absorption band	=C-H bend	Trans-RCH=CHR'
11.	723.1	Weak absorption band	-(CH_2)n bend	Alkanes and alkyls

Conclusions: Information and data provided on the surface properties of the catalyst prepared showed that the catalyst is mesoporous and has the potential to be used for catalytic reactions. The high yield of biodiesel indicate that waste vegetable oil is a potential low cost biobased feed stock for biodiesel formulations. The properties of biodiesel prepared from waste cooking oil compared reasonable well with the standards of biodiesel.

REFERENCES

Adefarati, FB (1986). Development of non-edible oils for use in the Nigerian surface coating industry with particular reference to rubber (*Hevea brasiliensis*) seed oil for the manufacture of air-drying oil-modified alkyds. In: Enabor, E.E. (Ed.), Industrial Utilisation of Natural Rubber (*Hevea brasiliensis*) Seed, Latex and Wood. Rubber Research Institute of Nigeria, Benin City, p. 27–38.

Aisabor, W; Lukman, Y; Otaru, AJ; Anakhu, AE; Otoikhian, SK (2016). Optimisation and Kinetics of Rubber Seed Oil Biodiesel Production. *J. Biofuels*, 7(2): 53-61.

Akhabue, CE; Osa-Benedict, EO; Oyedoh, EA; Otoikhian, SK (2020). Development of a bio-based bifunctional catalyst for simultaneous esterification and traansesterification of neem seed oil: Modeling and optimization studies. *Renewable Energy*, 152:724-735.

AOAC International (2000). Official Methods of Analysis of AOAC International 17th edn (Gaithersburg, MD: AOAC International)

ASTM (2008). Standard specification for biodiesel fuel (B100) blend stock for distillate fuels. In: Annual Book of ASTM Standards, ASTM International, West Conshohocken, Method D6751-08.

Boey, P; Maniama, GP; Abd Hamid, S (2011). Performance of calcium oxide as a heterogeneous catalyst in biodiesel production: A review. *Chem. Engineer. J.* 168: 15–22.

Bora, A; Dhawane, SH.; Anupam, K; Halder, G (2018). Biodiesel synthesis from Mesua ferrea oil using waste shell derived carbon catalyst. *Renewable Energy*, 121: 195–204.

Chandra, TC; Mirna, MM; Sunarso, J; Sudaryanto, Y; Ismadji, S (2009). "Activated carbon from durian shell: Preparation and characterization. *J. Taiwan Institute of Chemical Engineers*, 40: 457-462.

Choi, JM; Han, SK; Kim, JT; Lee, CY (2016). Optimization of combined (acid-thermal) pre-treatment for enhanced dark fermentative H_2 production from Chlorella vulgaris using response surface methodology. *Int. Biodeter. Biodegr.*, 108: 191-197.

Conceição, LRV; Reis, CER; de Lima, R; Cortez, DV; de Castro, HF. (2019). Keggin-structure heteropolyacid supported on alumina to be used in trans/esterification of high-acid feedstocks. *RSC Advances*, 9(41): 23450–23458

Deboni, T; Hirata, G; Shimamoto, GG; Tubino, M; de Almeida, M, Antonio J (2017). Deacidification and ethyl biodiesel production from acid soybean oil using a strong anion exchange resin. *Chem. Engineer. J.* S1385894717316066.

Dhawane, SH; Kumar, TL Halder, G (2018). Recent advancement and prospective of heterogeneous carbonaceous catalysts in chemical and enzymatic transformation of biodiesel. *Energy Convers. Manage*. 167: 176–202,

Ekwu, FC ; Nwagu, A (2004). Effect of processing on the quality of cashew nut oils. *J. Sci. Agric. Food Tech. Environ*., 4:105– 110.

Hidayu, AR; Muda, N (2016). Preparation and characterization of impregnated activated carbon from palm kernel shell and coconut shell for CO_2 capture. *P. Eng*., 148:106-113.

Jabeen, H; Iqbal, S; Anwar, S; Parales, RE (2015). Optimization of profenofos degradation by a novel bacterial consortium PBAC using response surface methodology. *Int. Biodeter. Biodegr*. 100:89-97.

Kalderis, D; Bethanis, S; Paraskeva, P; Daimadopulos, E (2008). Production of activated carbon from bagasse and rice husk by single-stage chemical activation method at low retention times. *Bioresource Technol.* 99:6809-6816.

Kour, D; Rana, KL; Yadav, N; Yadav, AJ; Rastegari, AA; Singh, C; Negi, P; Singh, K; Saxena, AK (2019). Technologies for Biofuel Production: Current Development, Challenges, and Future Prospects. *Prospects of Renewable Bioprocessing in Future Energy Systems*, 1-50.

Li, W; Sun, L; Xie, L; Deng, X; Naijia Guan, N; Li, L (2019). Review (Special Issue on Celebrating the 100th Anniversary of Nankai University) coordinately unsaturated sites in zeolite matrix: Construction and catalysis. *Chinese J. Catalysis*, 40:1255–1281.

Maneerung, TL; Kawi, S; Dai, Y; Wang, C (2016). Sustainable biodiesel production via transesterification of waste cooking oil by using CaO catalysts prepared from chicken manure. *Energy Convers. Manage*. 123: 487–497.

Mitaphonna, R; Ramli, M; Maulana, I; Novita, D; Zahara, I; Wardani, R. (2019). Preparation of Heterogenous Catalyst of Aceh Cow Bone Material and its Catalytic Performance for Biodiesel Synthesis. *International Proceeding Asean Youth Conference 2018 PPI-MALAYSIA*, ISSN: 2599-2643

Mohd Iqbaldin, MN; Azlan, MIM; Zaidi, AG; Surani, B; Zubri, Bz (2013). Properties of coconut shell activated carbon. *J. Trop. Forest Sci*. 25(4): 497–503.

Niu, S; Ning, Y; Lu, C; Han, K; Yu, H; Zhou, Y (2018). Esterification of oleic acid to produce biodiesel catalyzed by sulfonated activated carbon from bamboo. *Energy Conversion and Manage.* 163: 59–65.

Phan, A and Phan, TM (2008). Biodiesel production from waste cooking oils. *Fuel*, 87(17–18): 3490-3496.

Prauchner, MJ; Roriguez-reinoso, F (2012). Chemical versus physical activation of coconut shell: a comparative study. *Micropor. Mesopor. Mater*. 152:163-171.

Quah, RV; Tan, YH; Mujawar, MN; Nolasco-Hipolito, C; Khalid, M; Abdulah, EC (2019). An overview of biodiesel production using recyclable biomass and non-biomass derived magnetic catalysts. *J. Environ. Chem. Engineer.* 7(4):103219.

Saeed, RH; Kassem, Y; Çamur, H (2019). Effect of biodiesel mixture derived from waste frying-corn, frying-canola-corn and canola-corn cooking oils with various ages on physicochemical properties. *Energies*. 12(19): 3729.

Salimon, J; Abdullah, BM; Salih, N (2012). Saponification of *Jatropha curcas* seed oil: optimization by D-optimal design. *Inter. J. Chem. Engineer.* ID574780:1-6.

Sani, YM; Raji, AO; Alaba, PA; Abdul Aziz, AR; Wan Daud, WMA (2015). Palm catalysts for biodiesel. *Bioresources*, 10(2):3394-3408.

Suresh, M; Jawahar, CP; Richard, A (2018). A review on biodiesel production, combustion, performance, and emission characteristics of non-edible oils in variable compression ratio diesel engine using biodiesel and its blends. *Renewable and Sustainable Energy Reviews*, 92: 38-49.

Tabaraki, R; Nateghi, A; Ahmady-Asbchin, S (2014). Biosorption of lead (II) ions sargassum ilicifolium: application of response surface methodology. *Int. Biodeter. Biodegr*., 93:145-152.

Thushari, I; Babel, S (2018). Sustainable utilization of waste palm oil and sulfonated carbon catalyst derived from Coconut meal residue for biodiesel production. *Bioresour. Technol*., 248: 199–203.

Uddin, MK; Ferdous, K; Uddin, MR; Khan, MR; Islam, MA (2013). Synthesis of Biodiesel from Waste Cooking Oil. *Chemical Engineering and Science*, 1(2): 22-26.

Wang, H; Liu, L; Gong, S (2017). Esterification of oleic acid to biodiesel over a 12-phosphotungstic acid-based solid catalyst. *J. Fuel Chem. Technol*., 45: 303–310

Witek-Krowiak, A; Chojnacka, K; Podstawczyk, D; Dawiec, A; Pokomeda, K (2014). Application of response surface methodology and artificial neural network in modelling and optimization of biosorption process. *Bioresour. Technol*., 160:150-160.

Xie, W; Li, H (2006). Alumina-supported potassium iodide as a heterogeneous catalyst for biodiesel production from soybean oil. *J. Mol. Catal. A: Chem*., 255: 1–9.

Zhang, Q; Li, H; Yang, S (2018). Facile and Low-cost Synthesis of Mesoporous Ti–Mo Bi-metal Oxide Catalysts for Biodiesel Production from Esterification of Free Fatty Acids in Jatropha curcas Crude Oil. *J. Oleo Sci*., 67: 579–588.

Zhang, Y; Wong, WT; Yung, KF (2014). Biodiesel production via esterification of oleic acid catalyzed by chlorosulfonic acid modified zirconia. *Appl. Energy*, 116:191–198.

Zhou, Y; Niu, S; Li, H (2016). Activity of the carbon-based heterogeneous acid catalyst derived from bamboo in esterification of oleic acid with ethanol. *J. Energy Convers. Manage*. 114: 188–196